

Decay constants and radiative decays of heavy mesons in light-front quark model

Ho-Meoyng Choi

Department of Physics, Teachers College, Kyungpook National University, Daegu, Korea 702-701

(Received 31 January 2007; published 23 April 2007)

We investigate the magnetic dipole decays $V \rightarrow P\gamma$ of various heavy-flavored mesons such as $(D, D^*, D_s, D_s^*, \eta_c, J/\psi)$ and $(B, B^*, B_s, B_s^*, \eta_b, Y)$ using the light-front quark model constrained by the variational principle for the QCD-motivated effective Hamiltonian. The momentum dependent form factors $F_{VP}(q^2)$ for $V \rightarrow P\gamma^*$ decays are obtained in the $q^+ = 0$ frame and then analytically continued to the timelike region by changing \mathbf{q}_\perp to $i\mathbf{q}_\perp$ in the form factors. The coupling constant $g_{VP\gamma}$ for real photon case is then obtained in the limit as $q^2 \rightarrow 0$, i.e. $g_{VP\gamma} = F_{VP}(q^2 = 0)$. The weak decay constants of heavy pseudoscalar and vector mesons are also calculated. Our numerical results for the decay constants and radiative decay widths for the heavy-flavored mesons are overall in good agreement with the available experimental data as well as other theoretical model calculations.

DOI: [10.1103/PhysRevD.75.073016](https://doi.org/10.1103/PhysRevD.75.073016)

PACS numbers: 13.40.Gp, 12.38.Lg, 13.20.He

I. INTRODUCTION

The physics of exclusive heavy meson decays has provided very useful testing ground for the precise determination of the fundamental parameters of the standard model (SM) and the development of a better understanding of the QCD dynamics. While the experimental tests of exclusive heavy meson decays are much easier than those of inclusive one, the theoretical understanding of exclusive decays is complicated mainly due to the nonperturbative hadronic matrix elements entered in the long distance nonperturbative contributions. Since a rigorous field-theoretic formulation with a first principle application of QCD to make a reliable estimates of the nonperturbative hadronic matrix elements has not so far been possible, most of theoretical efforts have been devoted to looking for phenomenological approaches to nonperturbative QCD dynamics.

Along with various exclusive processes such as leptonic, semileptonic and rare decays of heavy mesons, the one-photon radiative decays from the low-lying heavy vector (V) to heavy pseudoscalar (P) mesons, i.e. magnetic dipole $V(1^3S_1) \rightarrow P(1^1S_0)\gamma$ transitions, have been considered as a valuable testing ground to pin down the best phenomenological model of hadrons. For example, the calculations of $D^* \rightarrow D\gamma$ and $B^* \rightarrow B\gamma$ radiative decays have been investigated by various theoretical approaches, such as the quark model [1–5], light cone QCD sum rules [6,7], heavy quark effective theory (HQET) [8,9], cloudy bag model (CBM) [10], and chiral perturbation theory [11]. Recently, the radiative decays between two heavy quarkonia such as $J/\psi \rightarrow \eta_c\gamma$ and $Y \rightarrow \eta_b\gamma$ have also been studied by the potential nonrelativistic QCD (pNRQCD) [12] and relativistic quark model [13,14] approaches. In our previous light-front quark model (LFQM) analysis [15–17] based on the QCD-motivated effective Hamiltonian, we have analyzed various exclusive processes such as the $0^- \rightarrow 0^-$ semileptonic heavy meson decays [16], rare $B \rightarrow Kl^+l^-$ ($l = e, \mu, \tau$) decays, and radiative

$V \rightarrow P\gamma$ and $P \rightarrow V\gamma$ decays of light-flavored mesons ($\pi, \rho, \omega, K, K^*, \phi, \eta, \eta'$) [15] and found a good agreement with the experimental data.

The main purpose of this work is to investigate the magnetic dipole transition $V \rightarrow P\gamma$ for the heavy-flavored mesons such as $(D, D^*, D_s, D_s^*, \eta_c, J/\psi)$ and $(B, B^*, B_s, B_s^*, \eta_b, Y)$ using our LFQM [15–17]. Since the experimental data available in this heavy-flavored sector are scanty, predictions of a model, if found reliable, can be utilized quite fruitfully. In addition, we calculate the weak decay constants of heavy pseudoscalar and vector mesons, which play important roles in many aspects, such as in the determination of Cabibbo-Kobayashi-Maskawa matrix elements, in the leptonic or nonleptonic weak decays of mesons, and in the neutral $D - \bar{D}$ or $B - \bar{B}$ mixing process, etc. Our LFQM [15–17] used in the present analysis has a couple of salient features compared to other LFQM [3,13] analyses: (1) We have implemented the variational principle to QCD-motivated effective LF Hamiltonian to enable us to analyze the meson mass spectra and to find optimized model parameters, which are to be used subsequently in the present investigation. Such an approach can better constrain the phenomenological parameters and establish the extent of applicability of our LFQM to wider ranging hadronic phenomena. (2) We have performed the analytic continuation from the spacelike ($q^2 < 0$) region to the physical timelike region [$0 \leq q^2 \leq (M_V - M_P)^2$] to obtain the decay form factors $F_{VP}(q^2)$ for $V \rightarrow P\gamma^*$ transitions. The Drell-Yan-West ($q^+ = q^0 + q^3 = 0$) frame is useful because only valence contributions are needed, i.e. the hadronic matrix element $\langle P | J_{em}^\mu | V \rangle$ is represented as the overlap of valence wave function, as far as the “ $\mu = +$ ” component of the current is used.

The paper is organized as follows: In Sec. II, we briefly describe the formulation of our LFQM [15,16] and the procedure of fixing the model parameters using the variational principle for the QCD-motivated effective Hamiltonian. The decay constants and radiative $V \rightarrow P\gamma$ decay widths for heavy-flavored mesons are then uniquely deter-

mined in our model calculation. In Sec. III, the formulas for the decay constants of pseudoscalar and vector mesons as well as the decay widths for $V \rightarrow P\gamma$ in our LFQM are given. To obtain the q^2 -dependent transition form factors $F_{VP}(q^2)$ for $V \rightarrow P\gamma^*$ transitions, we use the $q^+ = 0$ frame (i.e. $q^2 = -\mathbf{q}_\perp^2 < 0$) and then analytically continue the spacelike results to the timelike $q^2 > 0$ region by changing \mathbf{q}_\perp to $i\mathbf{q}_\perp$ in the form factor. The coupling constants $g_{VP\gamma}$ needed for the calculations of the decay widths for $V \rightarrow P\gamma$ can then be determined in the limit as $q^2 \rightarrow 0$, i.e. $g_{VP\gamma} = F_{VP}(q^2 = 0)$. In Sec. IV, we present our numerical results and compare with the available experimental data as well as other theoretical model predictions. Summary and conclusions follow in Sec. V.

II. MODEL DESCRIPTION

The key idea in our LFQM [15,16] for mesons is to treat the radial wave function as trial function for the variational principle to the QCD-motivated effective Hamiltonian saturating the Fock state expansion by the constituent quark and antiquark. The QCD-motivated Hamiltonian for a description of the ground state meson mass spectra is given by

$$\begin{aligned} H_{q\bar{q}}|\Psi_{nlm}^{JJ_z}\rangle &= [\sqrt{m_q^2 + \vec{k}^2} + \sqrt{m_{\bar{q}}^2 + \vec{k}^2} + V_{q\bar{q}}]|\Psi_{nlm}^{JJ_z}\rangle \\ &= [H_0 + V_{q\bar{q}}]|\Psi_{nlm}^{JJ_z}\rangle = M_{q\bar{q}}|\Psi_{nlm}^{JJ_z}\rangle, \end{aligned} \quad (1)$$

where $\vec{k} = (\mathbf{k}_\perp, k_z)$ is the three-momentum of the constituent quark, $M_{q\bar{q}}$ is the mass of the meson, and $|\Psi_{nlm}^{JJ_z}\rangle$ is the meson wave function. In this work, we use two interaction potentials $V_{q\bar{q}}$ for the pseudoscalar (0^{-+}) and vector (1^{--}) mesons: (1) Coulomb plus harmonic oscillator (HO), and (2) Coulomb plus linear confining potentials. In addition, the hyperfine interaction, which is essential to distinguish vector from pseudoscalar mesons, is included for both cases, viz.,

$$\begin{aligned} V_{q\bar{q}} &= V_0 + V_{\text{hyp}} \\ &= a + \mathcal{V}_{\text{conf}} - \frac{4\alpha_s}{3r} + \frac{2}{3} \frac{\mathbf{S}_q \cdot \mathbf{S}_{\bar{q}}}{m_q m_{\bar{q}}} \nabla^2 V_{\text{coul}}, \end{aligned} \quad (2)$$

where $\mathcal{V}_{\text{conf}} = br(r^2)$ for the linear (HO) potential and $\langle \mathbf{S}_q \cdot \mathbf{S}_{\bar{q}} \rangle = 1/4(-3/4)$ for the vector (pseudoscalar) meson.

The momentum space light-front wave function of the ground state pseudoscalar and vector mesons is given by

$$\Psi_{100}^{JJ_z}(x_i, \mathbf{k}_{i\perp}, \lambda_i) = \mathcal{R}_{\lambda_1 \lambda_2}^{JJ_z}(x_i, \mathbf{k}_{i\perp}) \phi(x_i, \mathbf{k}_{i\perp}), \quad (3)$$

where $\phi(x_i, \mathbf{k}_{i\perp})$ is the radial wave function and $\mathcal{R}_{\lambda_1 \lambda_2}^{JJ_z}$ is the spin-orbit wave function, which is obtained by the interaction independent Melosh transformation from the ordinary equal-time static spin-orbit wave function assigned by the quantum numbers J^{PC} . The model wave

function in Eq. (3) is represented by the Lorentz-invariant variables, $x_i = p_i^+/P^+$, $\mathbf{k}_{i\perp} = \mathbf{p}_{i\perp} - x_i \mathbf{P}_\perp$ and λ_i , where $P^\mu = (P^+, P^-, \mathbf{P}_\perp) = (P^0 + P^3, (M^2 + \mathbf{P}_\perp^2)/P^+, \mathbf{P}_\perp)$ is the momentum of the meson M , p_i^μ and λ_i are the momenta and the helicities of constituent quarks, respectively.

The covariant forms of the spin-orbit wave functions for pseudoscalar and vector mesons are given by

$$\begin{aligned} \mathcal{R}_{\lambda_1 \lambda_2}^{00} &= \frac{-\bar{u}(p_1, \lambda_1) \gamma_5 v(p_2, \lambda_2)}{\sqrt{2} \tilde{M}_0}, \\ \mathcal{R}_{\lambda_1 \lambda_2}^{1J_z} &= \frac{-\bar{u}(p_1, \lambda_1) [\not{\epsilon}(J_z) - \frac{\epsilon \cdot (p_1 - p_2)}{M_0 + m_1 + m_2}] v(p_2, \lambda_2)}{\sqrt{2} \tilde{M}_0}, \end{aligned} \quad (4)$$

where $\tilde{M}_0 = \sqrt{M_0^2 - (m_1 - m_2)^2}$ and M_0^2 is the invariant meson mass square M_0^2 defined as

$$M_0^2 = \sum_{i=1}^2 \frac{\mathbf{k}_{i\perp}^2 + m_i^2}{x_i}. \quad (5)$$

The polarization vectors $\epsilon^\mu(J_z)$ of the vector meson with four momentum P are given by

$$\begin{aligned} \epsilon^\mu(\pm 1) &= \left[0, \frac{2}{P^+} \epsilon_\perp(\pm) \cdot \mathbf{P}_\perp, \epsilon_\perp(\pm 1) \right], \\ \epsilon_\perp(\pm 1) &= \mp \frac{(1, \pm i)}{\sqrt{2}}, \\ \epsilon^\mu(0) &= \frac{1}{M_0} \left[P^+, \frac{\mathbf{P}_\perp^2 - M_0^2}{P^+}, \mathbf{P}_\perp \right]. \end{aligned} \quad (6)$$

The spin-orbit wave functions satisfy the following relations

$$\sum_{\lambda_1 \lambda_2} \mathcal{R}_{\lambda_1 \lambda_2}^{JJ_z \dagger} \mathcal{R}_{\lambda_1 \lambda_2}^{JJ_z} = 1, \quad (7)$$

for both pseudoscalar and vector mesons. For the radial wave function ϕ , we use the same Gaussian wave function for both pseudoscalar and vector mesons

$$\phi(x_i, \mathbf{k}_{i\perp}) = \frac{4\pi^{3/4}}{\beta^{3/2}} \sqrt{\frac{\partial k_z}{\partial x}} \exp(-\vec{k}^2/2\beta^2), \quad (8)$$

where β is the variational parameter. When the longitudinal component k_z is defined by $k_z = (x - 1/2)M_0 + (m_2^2 - m_1^2)/2M_0$, the Jacobian of the variable transformation $\{x, \mathbf{k}_\perp\} \rightarrow \vec{k} = (\mathbf{k}_\perp, k_z)$ is given by

$$\frac{\partial k_z}{\partial x} = \frac{M_0}{4x_1 x_2} \left\{ 1 - \left[\frac{m_1^2 - m_2^2}{M_0^2} \right]^2 \right\}. \quad (9)$$

Note that the free kinetic part of the Hamiltonian $H_0 = \sqrt{m_q^2 + \vec{k}^2} + \sqrt{m_{\bar{q}}^2 + \vec{k}^2}$ is equal to the free mass operator M_0 in the light-front formalism.

The normalization factor in Eq. (8) is obtained from the following normalization of the total wave function,

TABLE I. The constituent quark mass [GeV] and the Gaussian parameters β [GeV] for the linear and HO potentials obtained by the variational principle. $q = u$ and d .

Model	m_q	m_s	m_c	m_b	β_{qc}	β_{sc}	β_{cc}	β_{qb}	β_{sb}	β_{bb}
Linear	0.22	0.45	1.8	5.2	0.468	0.502	0.651	0.527	0.571	1.145
HO	0.25	0.48	1.8	5.2	0.422	0.469	0.700	0.496	0.574	1.803

$$\int_0^1 dx \int \frac{d^2 \mathbf{k}_\perp}{16\pi^3} |\Psi_{100}^{JJ_z}(x, \mathbf{k}_{i\perp})|^2 = 1. \quad (10)$$

Our variational principle to the QCD-motivated effective Hamiltonian first evaluate the expectation value of the central Hamiltonian $H_0 + V_0$, i.e. $\langle \phi | (H_0 + V_0) | \phi \rangle$ with a trial function $\phi(x_i, \mathbf{k}_{i\perp})$ that depends on the variational parameters β and varies β until $\langle \phi | (H_0 + V_0) | \phi \rangle$ is a minimum. Once these model parameters are fixed, then, the mass eigenvalue of each meson is obtained by $M_{q\bar{q}} = \langle \phi | (H_0 + V_{q\bar{q}}) | \phi \rangle$. On minimizing energies with respect to β and searching for a fit to the observed ground state meson spectra, our central potential V_0 obtained from our optimized potential parameters ($a = -0.72$ GeV, $b = 0.18$ GeV², and $\alpha_s = 0.31$) [15] for Coulomb plus linear potential were found to be quite comparable with the quark potential model suggested by Scora and Isgur [18] where

they obtained $a = -0.81$ GeV, $b = 0.18$ GeV², and $\alpha_s = 0.3 \sim 0.6$ for the Coulomb plus linear confining potential. More detailed procedure of determining the model parameters of light and heavy quark sectors can be found in our previous works [15, 16]. Our model parameters (m, β) for the heavy quark sector obtained from the linear and HO potential models are summarized in Table I.

Our predictions of the ground state pseudoscalar and vector meson mass spectra obtained from the linear potential parameters were already shown in [16]. In this work, we include the results obtained from the HO potential parameters as well and summarize them in Fig. 1. Our predictions of the ground state meson mass spectra obtained from both linear and HO parameters agree with the experimental data [19] within 6% error. We should note that our previously predicted mass of B_s^* , $M_{B_s^*} = 5424[5471]$ MeV obtained from the linear [HO] parameters is in good agreement with the very recent CLEO data, $M_{B_s^*} = 5414 \pm 1 \pm 4$ MeV [20] and $M_{B_s^*} = 5411.7 \pm 1.6 \pm 0.6$ MeV [21]. For the experimentally unmeasured mass of η_b meson, our prediction of mass difference between the two bottomonia $\Delta m (= M_Y - M_{\eta_b}) = 34[263]$ MeV obtained from the linear [HO] parameters is consistent with current theoretical estimates (from perturbative QCD and lattice NRQCD), $\Delta m = 34 \sim 141$ MeV [22]. As we shall see in our numerical calculations, the radiative decay of $Y \rightarrow \eta_b \gamma$ might be useful to determine the mass of η_b experimentally since the decay width $\Gamma(Y \rightarrow \eta_b \gamma)$ is very sensitive to the value of Δm , viz. $\Gamma \propto (\Delta m)^3$.

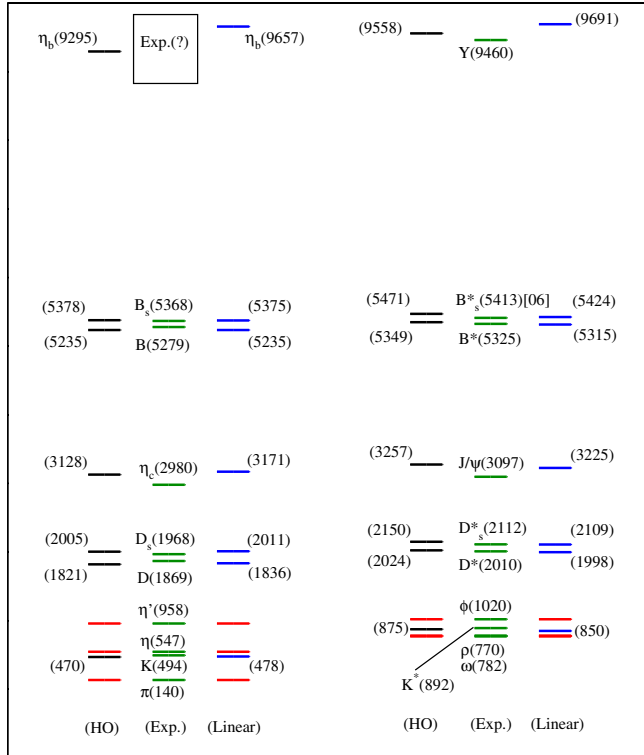


FIG. 1 (color online). Fit of the ground state meson masses [MeV] with the parameters given in Table I. The (ρ, π), (η, η'), and (ω, ϕ) masses are our input data. The masses of ($\omega - \phi$) and ($\eta - \eta'$) were used to determine the mixing angles of $\omega - \phi$ and $\eta - \eta'$ [15], respectively.

III. DECAY CONSTANTS AND RADIATIVE DECAY WIDTHS

The decay constants of pseudoscalar and vector mesons are defined by

$$\begin{aligned} \langle 0 | \bar{q} \gamma^\mu \gamma_5 q | P \rangle &= i f_P P^\mu, \\ \langle 0 | \bar{q} \gamma^\mu q | V(P, h) \rangle &= f_V M_V \epsilon^\mu(h), \end{aligned} \quad (11)$$

where the experimental value of vector meson decay constant f_V is extracted from the longitudinal ($h = 0$) polarization. In the above definitions for the decay constants, the experimental values of pion and rho meson decay constants are $f_\pi \approx 131$ MeV from $\pi \rightarrow \mu \nu$ and $f_\rho \approx 220$ MeV from $\rho \rightarrow e^+ e^-$.

Using the plus component ($\mu = +$) of the current, one can easily calculate the decay constants. The explicit forms

of pseudoscalar and vector meson decay constants are given by

$$f_P = 2\sqrt{6} \int \frac{dx d^2\mathbf{k}_\perp}{16\pi^3} \frac{\mathcal{A}}{\sqrt{\mathcal{A}^2 + \mathbf{k}_\perp^2}} \phi(x, \mathbf{k}_\perp),$$

$$f_V = 2\sqrt{6} \int \frac{dx d^2\mathbf{k}_\perp}{16\pi^3} \frac{\phi(x, \mathbf{k}_\perp)}{\sqrt{\mathcal{A}^2 + \mathbf{k}_\perp^2}} \left[\mathcal{A} + \frac{2\mathbf{k}_\perp^2}{\mathcal{M}_0} \right], \quad (12)$$

where $\mathcal{A} = x_2 m_1 + x_1 m_2$ and $\mathcal{M}_0 = M_0 + m_1 + m_2$.

In our LFQM calculation of $V \rightarrow P\gamma$ decay process, we shall first analyze the virtual photon (γ^*) decay process so that we calculate the momentum dependent transition form factor, $F_{VP}(q^2)$. The lowest-order Feynman diagram for $V \rightarrow P\gamma^*$ process is shown in Fig. 2 where the decay from vector meson to pseudoscalar meson and virtual photon state is mediated by a quark loop with flavors of constituent mass m_1 and m_2 .

The transition form factor $F_{VP}(q^2)$ for the magnetic dipole decay of vector meson $V(P) \rightarrow P(P')\gamma^*(q)$ is defined as

$$\langle P(P') | J_{\text{em}}^\mu | V(P, h) \rangle = ie \epsilon^{\mu\nu\rho\sigma} \epsilon_\nu(P, h) q_\rho P_\sigma F_{VP}(q^2), \quad (13)$$

where the antisymmetric tensor $\epsilon^{\mu\nu\rho\sigma}$ assures electromagnetic gauge invariance, $q = P - P'$ is the four momentum of the virtual photon, $\epsilon_\nu(P, h)$ is the polarization vector of the initial meson with four momentum P and helicity h . The kinematically allowed momentum transfer squared q^2 ranges from 0 to $q_{\text{max}}^2 = (M_V - M_P)^2$.

The decay form factor $F_{VP}(q^2)$ can be obtained in the $q^+ = 0$ frame with the ‘‘good’’ component of currents, i.e. $\mu = +$, without encountering zero-mode contributions [23]. Thus, we shall perform our LFQM calculation in the $q^+ = 0$ frame, where $q^2 = q^+ q^- - \mathbf{q}_\perp^2 = -\mathbf{q}_\perp^2 < 0$, and then analytically continue the form factor $F_{VP}(\mathbf{q}_\perp^2)$ in the spacelike region to the timelike $q^2 > 0$ region by changing \mathbf{q}_\perp to $i\mathbf{q}_\perp$ in the form factor.

The quark momentum variables for $V(q_1 \bar{q}_2) \rightarrow P(q'_1 \bar{q}'_2)$ transitions in the $q^+ = 0$ frame are given by

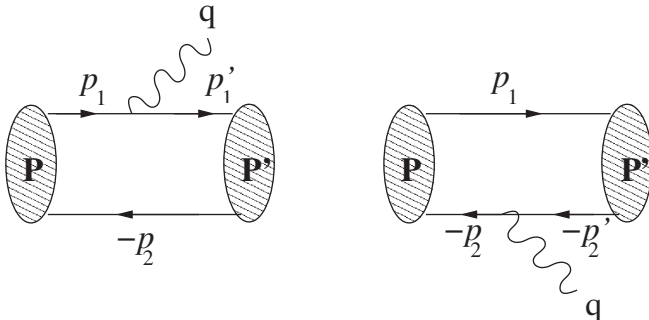


FIG. 2. Lowest order graph for $V \rightarrow P\gamma^*$ transitions.

$$p_1^+ = x_1 P^+, \quad p_2^+ = x_2 P^+, \quad \mathbf{p}_{1\perp} = x_1 \mathbf{P}_\perp + \mathbf{k}_\perp,$$

$$\mathbf{p}_{2\perp} = x_2 \mathbf{P}_\perp - \mathbf{k}_\perp, \quad p_1'^+ = x_1 P'^+, \quad p_2'^+ = x_2 P'^+,$$

$$\mathbf{p}'_{1\perp} = x_1 \mathbf{P}'_\perp + \mathbf{k}'_\perp, \quad \mathbf{p}'_{2\perp} = x_2 \mathbf{P}'_\perp - \mathbf{k}'_\perp, \quad (14)$$

where $x_1 = x$ and $x_2 = 1 - x$ and the spectator quark requires that $p_2^+ = p_2'^+$ and $\mathbf{p}_{2\perp} = \mathbf{p}'_{2\perp}$. In the calculations of the decay form factor $F_{VP}(q^2)$, we use ‘‘+’’-component of currents and the transverse ($h = \pm 1$) polarization. For the longitudinal ($h = 0$) polarization, it is hard to extract the form factor since both sides of Eq. (13) are vanishing for any q^2 value.

The hadronic matrix element of the plus current, $\langle J^+ \rangle = \langle P(P') | J_{\text{em}}^+ | V(P, h = +) \rangle$ in Eq. (13) is then obtained by the convolution formula of the initial and final state light-front wave functions:

$$\langle J^+ \rangle = \sum_j e e_j \int_0^1 \frac{dx}{16\pi^3} \int d^2\mathbf{k}_\perp \phi(x, \mathbf{k}'_\perp) \phi(x, \mathbf{k}_\perp)$$

$$\times \sum_{\lambda\lambda'} \mathcal{R}_{\lambda\lambda'}^{00\dagger} \frac{\bar{u}_{\lambda'}(p'_1)}{\sqrt{p_1'^+}} \gamma^+ \frac{u_\lambda(p_1)}{\sqrt{p_1^+}} \mathcal{R}_{\lambda\lambda'}^{11}, \quad (15)$$

where $\mathbf{k}'_\perp = \mathbf{k}_\perp - x_2 \mathbf{q}_\perp$ and $e e_j$ is the electrical charge for j th quark flavor. Comparing with the right-hand side of Eq. (13), i.e. $e P^+ F_{VP}(Q^2) q^R / \sqrt{2}$ where $q^R = q_x + i q_y$, we could extract the one-loop integral, $I(m_1, m_2, q^2)$, which is given by

$$I(m_1, m_2, q^2) = \int_0^1 \frac{dx}{8\pi^3} \int d^2\mathbf{k}_\perp \frac{\phi(x, \mathbf{k}'_\perp) \phi(x, \mathbf{k}_\perp)}{x_1 \tilde{M}_0 \tilde{M}'_0}$$

$$\times \left\{ \mathcal{A} + \frac{2}{\mathcal{M}_0} \left[\mathbf{k}_\perp^2 - \frac{(\mathbf{k}_\perp \cdot \mathbf{q}_\perp)^2}{\mathbf{q}_\perp^2} \right] \right\}, \quad (16)$$

where the primed factors are the functions of final state momenta, e.g. $\tilde{M}'_0 = \tilde{M}'_0(x, \mathbf{k}'_\perp)$.

Then, the decay form factor $F_{VP}(q^2)$ is obtained as

$$F_{VP}(q^2) = e_1 I(m_1, m_2, q^2) + e_2 I(m_2, m_1, q^2). \quad (17)$$

The coupling constant $g_{VP\gamma}$ for real photon (γ) case can then be determined in the limit as $q^2 \rightarrow 0$, i.e. $g_{VP\gamma} = F_{VP}(q^2 = 0)$. The decay width for $V \rightarrow P\gamma$ is given by

$$\Gamma(V \rightarrow P\gamma) = \frac{\alpha}{3} g_{VP\gamma}^2 k_\gamma^3, \quad (18)$$

where α is the fine-structure constant and $k_\gamma = (M_V^2 - M_P^2)/2M_V$ is the kinematically allowed energy of the outgoing photon.

IV. NUMERICAL RESULTS

In our numerical calculations, we use two sets of model parameters (m, β) for the linear and HO confining potentials given in Table I to perform, in a way, a parameter-free-calculation of decay constants and decay rates for heavy pseudoscalar and vector mesons. Although our predictions

of ground state heavy meson masses are overall in good agreement with the experimental values, we use the experimental meson masses in the computations of the radiative decay widths to reduce possible theoretical uncertainties. But in the case of η_b , for which experimental data is not yet available, we use the model mass as $M_{\eta_b} = 9353 \pm 50$ MeV, i.e. we use slightly broader range $\Delta m = M_Y - M_{\eta_b} = 60\text{--}160$ MeV than that reported in [22].

In Table II, we present our predictions for the charmed meson decay constants ($f_D, f_{D^*}, f_{D_s}, f_{D_s^*}, f_{\eta_c}, f_{J/\psi}$) together with lattice QCD [24,25], QCD sum rules [26], relativistic Bethe-Salpeter (BS) model [27], relativized quark model [28], and other relativistic quark model (RQM) [29] predictions as well as the available experimental data [19,30–32]. Note that we extract the experimental value $(f_{J/\psi})_{\text{exp}} = (416 \pm 6)$ MeV from the data $\Gamma_{\text{exp}}(J/\psi \rightarrow e^+e^-) = 5.55 \pm 0.14 \pm 0.02$ keV [19] and the formula [33]

$$\Gamma(V \rightarrow e^+e^-) = \frac{4\pi}{3} \frac{\alpha^2}{M_V} f_V^2 c_V, \quad (19)$$

where $c_V = 4/9$ for $V = J/\psi$. Our predictions for the ratios $f_{D_s}/f_D = 1.18[1.20]$ and $f_{\eta_c}/f_{J/\psi} = 0.91[0.90]$ obtained from the linear [HO] parameters are in good agreement with the available experimental data, $(f_{D_s}/f_D)_{\text{exp.}} = 1.27 \pm 0.12 \pm 0.03$ (preliminary) [31] and

$(f_{\eta_c}/f_{J/\psi})_{\text{exp.}} = 0.81 \pm 0.19$ [19,32], respectively. Our result for the ratio $f_{D_s^*}/f_{D^*} = 1.14[1.18]$ obtained from the linear [HO] parameters is also consistent with the quenched lattice result, 1.11 (3) [24] and the BS one, 1.10 ± 0.06 [27]. Overall, our results for the charmed meson decay constants are in good agreement with other theoretical model calculations as well as the experimental data.

In Table III, we show our results for the bottomed meson decay constants ($f_B, f_{B^*}, f_{B_s}, f_{B_s^*}, f_{\eta_b}, f_Y$) together with lattice QCD [24,34,35], QCD sum rules [26,36], BS model [27], relativized quark model [28], and RQM [29] predictions as well as the available experimental data [19,37]. Note that we extract the experimental value $(f_Y)_{\text{exp}} = (715 \pm 5)$ MeV from the data $\Gamma_{\text{exp}}(Y \rightarrow e^+e^-) = 1.340 \pm 0.018$ keV [19] and Eq. (19) with $c_V = 1/9$ for $V = Y$. Our results for the ratios $f_{B_s}/f_B = 1.24[1.32]$ and $f_{B_s^*}/f_{B^*} = 1.23[1.32]$ obtained from the linear [HO] parameters are quite comparable with the recent lattice results, 1.20(3)(1) [34] and $1.22^{(+5)}_{(-6)}$ [35] for $f_{B_s^*}/f_{B^*}$ and $1.17(4)^{+1}_{-3}$ [24] for f_{B_s}/f_{B^*} . For the Y meson decay constant, our prediction $f_Y = 529[893]$ MeV obtained from the linear [HO] parameters slightly deviates from the extracted experimental value $(f_Y)_{\text{exp}} = (715 \pm 5)$ MeV. Other model calculations for f_Y such as 498 ± 20 MeV from the BS model [27] and 836 MeV from effective Lagrangian satisfying heavy-quark spin symmetry

TABLE II. Charmed meson decay constants (in unit of MeV) obtained from the linear [HO] parameters.

	f_D	f_{D^*}	f_{D_s}	$f_{D_s^*}$	f_{η_c}	$f_{J/\psi}$
Linear [HO]	211[194]	254[228]	248[233]	290[268]	326[354]	360[395]
Lattice [24]	$211 \pm 14^{+2}_{-12}$	$245 \pm 20^{+3}_{-2}$	$231 \pm 12^{+8}_{-1}$	$272 \pm 16^{+3}_{-20}$	—	—
QCD [25]	$201 \pm 3 \pm 17$	—	$249 \pm 3 \pm 16$	—	—	—
Sum-rules [26]	204 ± 20	—	235 ± 24	—	—	—
BS [27]	230 ± 25	340 ± 23	248 ± 27	375 ± 24	292 ± 25	459 ± 28
QM [28]	240 ± 20	—	290 ± 20	—	—	—
RQM [29]	234	310	268	315	—	—
Exp.	$222.6 \pm 16.7^{+2.8}_{-3.4}$ [30]	—	$282 \pm 16 \pm 7$ [31]	—	335 ± 75 [32]	416 ± 6 [19]

TABLE III. Bottomed meson decay constants (in unit of MeV) obtained from the linear [HO] parameters.

	f_B	f_{B^*}	f_{B_s}	$f_{B_s^*}$	f_{η_b}	f_Y
Linear [HO]	189[180]	204[193]	234[237]	250[254]	507[897]	529[983]
Lattice [24]	$179 \pm 18^{+34}_{-9}$	$196 \pm 24^{+39}_{-2}$	$204 \pm 16^{+36}_{-0}$	$229 \pm 20^{+41}_{-16}$	—	—
QCD [34]	216 ± 22	—	259 ± 32	—	—	—
[35]	189 ± 27	—	230 ± 30	—	—	—
Sum-rules [36]	210 ± 19	—	244 ± 21	—	—	—
[26]	203 ± 23	—	236 ± 30	—	—	—
BS [27]	196 ± 29	238 ± 18	216 ± 32	272 ± 20	—	498 ± 20
QM [28]	155 ± 15	—	210 ± 20	—	—	—
RQM [29]	189	219	218	251	—	—
Exp.	229^{+36+34}_{-31-37} [37]	—	—	—	—	715 ± 5 [19]

(HQSS) [38] also show some deviations from the experimental value. Our result for the ratio $f_{\eta_b}/f_Y = 0.96[0.91]$ obtained from the linear [HO] parameters is to be compared with the $f_{\eta_b}/f_Y \sim 1$ in HQSS limit [38]. For these heavy bottomed meson decay constants, we observe an overall agreement between our results and other theoretical ones.

In Table IV, we present our results of the coupling constants $g_{VP\gamma}$ (in unit of GeV^{-1}) for radiative $V \rightarrow P\gamma$ decays together with other QM calculations [1–3] as well as the available experimental data. The experimental values for $(g_{J/\psi\eta_c\gamma})_{\text{exp}} = 0.57 \pm 0.11$ for $J/\psi \rightarrow \eta_c\gamma$ and $(g_{D^{*+}D^+\gamma})_{\text{exp}} = -(0.50 \pm 0.12)$ for $D^{*+} \rightarrow D^+\gamma$ processes are extracted from the branching ratios $\text{Br}(J/\psi \rightarrow \eta_c\gamma)_{\text{exp}} = (1.3 \pm 0.4)\%$ and $\text{Br}(D^{*+} \rightarrow D^+\gamma)_{\text{exp}} = (1.6 \pm 0.4)\%$ together with the full widths of $\Gamma_{\text{tot}}(J/\psi) = 93.4 \pm 2.1$ keV and $\Gamma_{\text{tot}}(D^{*+}) = 96 \pm 22$ keV [19]. The opposite sign of coupling constants for D^{*+} and D_s^{*+} decays compared to the charmonium J/ψ decay indicates that the charmed quark contribution is largely destructive in the radiative decays of D^{*+} and D_s^{*+} mesons. Similarly, we see that the bottomed quark contribution is largely destructive in the radiative decay of B^{*+} meson. Our predictions for $g_{J/\psi\eta_c\gamma} = 0.681[0.673]$ and $g_{D^{*+}D^+\gamma} = -0.384[-0.398]$ obtained from the linear [HO] parameters fall within the experimental error bars. Our result for the coupling constant ratio $|\frac{g_{D^{*0}D^0\gamma}}{g_{D^{*+}D^+\gamma}}| = 4.64[4.59]$ obtained from the linear [HO] parameters is quite comparable with other theoretical model predictions such as those 6.32 ± 2.97 [6] and 3.05 ± 0.63 [7] from the QCD sum rules, 5.54 ± 3.00 [9] from the heavy quark effective theory (HQET), and 4.49 ± 0.96 [39] from the broken-SU(4) symmetry by M1 transition. Incidentally, our result for the coupling constant ratio $|\frac{g_{B^{*0}B^0\gamma}}{g_{B^{*+}B^+\gamma}}| = 0.57[0.57]$ obtained from the linear [HO] parameters is the same as that from the other QM predictions [1–3]. This result is also com-

parable with 0.64 ± 0.51 [6] and 0.49 ± 0.38 [7] from the QCD sum rules, and 0.59 ± 0.48 [9] from the HQET.

We show in Fig. 3 our results of decay form factors $F_{VP}(q^2)$ obtained from the linear parameters. Since the results from the HO parameters are not much different from those of linear ones, we omit them for simplicity. The left (right) panel shows the results of charmed (bottomed) vector meson radiative $V \rightarrow P\gamma^*$ decays. The solid, dotted, dashed, and dot-dashed lines in the left (right) panel represent the form factors for $D^{*+} \rightarrow D^+\gamma^*(B^{*+} \rightarrow B^+\gamma^*)$, $D^{*0} \rightarrow D^0\gamma^*(B^{*0} \rightarrow B^0\gamma^*)$, $D_s^{*+} \rightarrow D_s^+\gamma^*(B_s^{*0} \rightarrow B_s^0\gamma^*)$, and $J/\psi \rightarrow \eta_c\gamma^*(Y \rightarrow \eta_b\gamma^*)$ decays, respectively. The arrows in the figure represent the zero recoil points of the final state pseudoscalar meson, i.e. $q^2 = q_{\text{max}}^2 = (M_V - M_P)^2$. We have performed the analytical continuation of the decay form factors $F_{VP}(q^2)$ from the spacelike region ($q^2 < 0$) to the physical timelike region $0 \leq q^2 \leq q_{\text{max}}^2$. The coupling constant $g_{VP\gamma}$ at $q^2 = 0$ corresponds to a final state pseudoscalar meson recoiling with maximum three-momentum $|\vec{P}_P| = (M_V^2 - M_P^2)/2M_V$ in the rest frame of vector meson. Because of the small kinematic region $0 \leq q^2 \leq q_{\text{max}}^2$ for the bottomed and bottomonium meson decays, the recoil effects of the final state mesons are quite negligible, i.e. $F_{VP}(q_{\text{max}}^2)/g_{VP\gamma} \approx 1$. Likewise, we find that $F_{J/\psi\eta_c}(q_{\text{max}}^2)/g_{J/\psi\eta_c\gamma} \approx F_{D_s^*D_s}(q_{\text{max}}^2)/g_{D_s^*D_s\gamma} \approx 1$ for $J/\psi \rightarrow \eta_c\gamma^*$ and $D_s^{*+} \rightarrow D_s^+\gamma^*$ decays. On the other hand, we obtain $F_{D^{*+}D^+}(q_{\text{max}}^2)/g_{D^{*+}D^+\gamma} = 0.420/0.384 \approx 1.1$ and $F_{D^{*0}D^0}(q_{\text{max}}^2)/g_{D^{*0}D^0\gamma} = 1.859/1.783 \approx 1.04$ for $D^{*+} \rightarrow D^+\gamma^*$ and $D^{*0} \rightarrow D^0\gamma^*$ decays, respectively. The recoil effect, i.e. the difference between the zero (q_{max}^2) and the maximum ($q^2 = 0$) points, may not be negligible especially for the $D^{*+} \rightarrow D^+\gamma^*$ decay. Figure 3 also shows the restoration of SU(3) flavor symmetry, $F_{D_s^*D_s^+}(q^2)/F_{D^{*+}D^+}(q^2) \rightarrow 1$ between charmed and charmed-strange mesons and $F_{B_s^*B_s^0}(q^2)/F_{B^{*0}B^0}(q^2) \rightarrow 1$ between bottomed and bottomed-strange mesons in the

TABLE IV. Coupling constants $g_{VP\gamma}$ [GeV^{-1}] for radiative $V \rightarrow P\gamma$ decays obtained from the linear [HO] parameters.

Coupling	This work	[3]	[2]	[1]	Exp. [19]
$g_{J/\psi\eta_c\gamma}$	0.681[0.673]	—	—	0.69	0.57 ± 0.11
$g_{D^{*+}D^+\gamma}$	$-0.384[-0.398]$	-0.30	-0.37	-0.35	$-(0.50 \pm 0.12)$
$g_{D^{*0}D^0\gamma}$	1.783[1.826]	1.85	1.94	1.78	—
$ \frac{g_{D^{*0}D^0\gamma}}{g_{D^{*+}D^+\gamma}} $	4.64[4.59]	6.17	5.24	5.08	—
$g_{D_s^{*+}D_s^+\gamma}$	$-0.167[-0.161]$	—	-0.17	-0.13	—
$g_{B^{*+}B^+\gamma}$	1.311[1.313]	1.40	1.50	1.37	—
$g_{B^{*0}B^0\gamma}$	$-0.749[-0.750]$	-0.80	-0.85	-0.78	—
$ \frac{g_{B^{*0}B^0\gamma}}{g_{B^{*+}B^+\gamma}} $	0.57[0.57]	0.57	0.57	0.57	—
$g_{B_s^{*0}B_s^0\gamma}$	$-0.553[-0.536]$	—	-0.62	-0.55	—
$g_{Y\eta_b\gamma}$	$-0.124[-0.119]$	—	—	-0.13	—

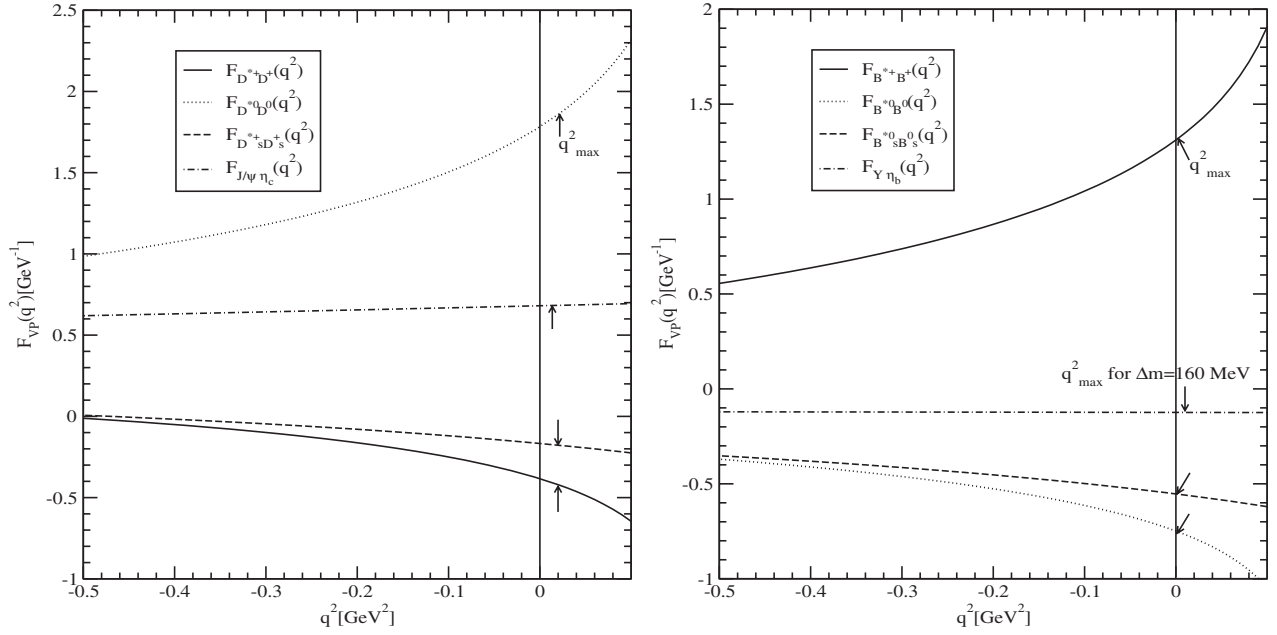


FIG. 3. Transition form factors $F_{VP}(q^2)$ for charmed (left panel) and bottomed (right panel) mesons radiative decays obtained from the linear parameters.

intermediate and deep spacelike ($q^2 < 0$) region, where the light quark current contribution becomes negligible.

For a more direct comparison with the available experimental data, we finally calculate the partial decay widths from Eq. (18). In Table V, we present our results for the decay widths and branching ratios together with the available experimental data. The errors in our results for the decay widths and branching ratios come from the uncertainties of the experimental mass values and experimental mass values plus the full widths, respectively. Our results of the branching ratios $\text{Br}(J/\psi \rightarrow \eta_c \gamma) = 1.80 \pm 0.10[1.76 \pm 0.10]\%$ and $\text{Br}(D^{*+} \rightarrow D^+ \gamma) = 0.93 \pm 0.31[1.00 \pm 0.34]\%$ obtained from the linear [HO] parameters are in agreement with the experimental data [19], $\text{Br}(J/\psi \rightarrow \eta_c \gamma)_{\text{exp}} = (1.3 \pm 0.4)\%$ and $\text{Br}(D^{*+} \rightarrow D^+ \gamma)_{\text{exp}} = (1.6 \pm 0.4)\%$ within the error bars. For the neutral charmed meson decay, our prediction $\Gamma(D^{*0} \rightarrow D^0 \gamma) = 20.0 \pm 0.3[21.0 \pm 0.3]$ keV obtained from the

linear [HO] parameters is to be compared with other theoretical model results such as 21.69 keV from the RQM [3], 14.40 keV from the QCD sum rules [7] and 27.0 ± 1.8 keV from broken-SU(4) symmetry by M1 transition [39]. For the charmed-strange meson decay, our prediction $\Gamma(D_s^{*+} \rightarrow D_s^+ \gamma) = 0.18 \pm 0.01[0.17 \pm 0.01]$ keV obtained from the linear [HO] parameters is comparable with other theoretical model results such as 0.19 keV from the RQM [5] and 0.3 keV [8] and (0.24 ± 0.24) keV [9] from the HQET. Since the D^{*0} lifetime has not been measured yet, we also try to estimate the full width for D^{*0} meson using the relation

$$\frac{\text{Br}(D^{*+} \rightarrow D^+ \gamma)}{\text{Br}(D^{*0} \rightarrow D^0 \gamma)} = \frac{\Gamma(D^{*+} \rightarrow D^+ \gamma) \Gamma_{\text{tot}}(D^{*0})}{\Gamma(D^{*0} \rightarrow D^0 \gamma) \Gamma_{\text{tot}}(D^{*+})}, \quad (20)$$

where we use our predicted decay width $\Gamma(D^{*0} \rightarrow D^0 \gamma)$ to extract the full width for D^{*0} . Similarly, we can estimate the full width for D_s^{*+} meson using the same method as in

TABLE V. Decay widths and branching ratios for radiative $V \rightarrow P\gamma$ decays obtained from our linear [HO] model parameters. We used $M_{\eta_b} = 9353 \pm 50$ MeV for $\Upsilon \rightarrow \eta_b \gamma$ decay.

Decay mode	Γ [keV]	Br	Br_{exp} [19]
$J/\psi \rightarrow \eta_c \gamma$	$1.69 \pm 0.05[1.65 \pm 0.05]$	$(1.80 \pm 0.10)[1.76 \pm 0.10]\%$	$(1.3 \pm 0.4)\%$
$D^{*+} \rightarrow D^+ \gamma$	$0.90 \pm 0.02[0.96 \pm 0.02]$	$(0.93 \pm 0.31)[1.00 \pm 0.34]\%$	$(1.6 \pm 0.4)\%$
$D^{*0} \rightarrow D^0 \gamma$	$20.0 \pm 0.3[21.0 \pm 0.3]$	—	$(38.1 \pm 2.9)\%$
$D_s^{*+} \rightarrow D_s^+ \gamma$	$0.18 \pm 0.01[0.17 \pm 0.01]$	—	$(94.2 \pm 0.7)\%$
$B^{*+} \rightarrow B^+ \gamma$	$0.40 \pm 0.03[0.40 \pm 0.03]$	—	—
$B^{*0} \rightarrow B^0 \gamma$	$0.13 \pm 0.01[0.13 \pm 0.01]$	—	—
$B_s^{*0} \rightarrow B_s^0 \gamma$	$0.068 \pm 0.017[0.064 \pm 0.016]$	—	—
$\Upsilon \rightarrow \eta_b \gamma$	$0.045^{+0.097}_{-0.038}[0.042^{+0.088}_{-0.036}]$	$(8.4^{+18.6}_{-7.2})[7.7^{+17.0}_{-6.6}] \times 10^{-4}$	—

the case of D^{*0} meson. Our averaged values of the full widths for D^{*0} and D_s^{*+} mesons obtained from the two parameter sets are

$$\begin{aligned}\Gamma_{\text{tot}}(D^{*0}) &= (55 \pm 6) \text{ keV}, \\ \Gamma_{\text{tot}}(D_s^{*+}) &= (0.19 \pm 0.01) \text{ keV},\end{aligned}\quad (21)$$

respectively, while experimentally only upper limits were reported as $\Gamma(D^{*0})_{\text{exp}} < 2.1 \text{ MeV}$ and $\Gamma(D_s^{*+})_{\text{exp}} < 1.9 \text{ MeV}$. Some other theoretical model predictions of the full widths for D^{*0} and D_s^{*+} mesons were also reported as $\Gamma_{\text{tot}}(D^{*0}) = 65.09 \text{ keV}$ from the RQM [3] and $\Gamma_{\text{tot}}(D^{*0}) = (36.7 \pm 9.7) \text{ keV}$ and $\Gamma_{\text{tot}}(D_s^{*+}) = (0.24 \pm 0.24) \text{ keV}$ from the HQET [9].

For B^* and B_s^* radiative decays, our results for the decay widths $\Gamma(B^{*+} \rightarrow B^+ \gamma) = 0.40 \pm 0.03[0.40 \pm 0.03]$, $\Gamma(B^{*0} \rightarrow B^0 \gamma) = 0.13 \pm 0.01[0.13 \pm 0.01]$, and $\Gamma(B_s^{*0} \rightarrow B_s^0 \gamma) = 0.068 \pm 0.017[0.064 \pm 0.016]$ obtained from the linear [HO] parameters are quite comparable with other theoretical model predictions such as $\Gamma(B^{*+} \rightarrow B^+ \gamma) = 0.429 \text{ keV}$ and $\Gamma(B^{*0} \rightarrow B^0 \gamma) = 0.142 \text{ keV}$ from the RQM [3], $\Gamma(B^{*+} \rightarrow B^+ \gamma) = (0.22 \pm 0.09) \text{ keV}$ and $\Gamma(B^{*0} \rightarrow B^0 \gamma) = (0.075 \pm 0.027) \text{ keV}$ from the HQET [9], and $\Gamma(B^{*+} \rightarrow B^+ \gamma) = 0.14 \text{ keV}$ and $\Gamma(B^{*0} \rightarrow B^0 \gamma) = 0.09 \text{ keV}$ from the chiral perturbation theory [11]. Finally, for the $Y \rightarrow \eta_b \gamma$ process, our predictions for the decay width and branching ratio obtained from the linear [HO] parameters are $\Gamma(Y \rightarrow \eta_b \gamma) = 45_{-38}^{+97}[42_{-36}^{+88}] \text{ eV}$ and $\text{Br}(Y \rightarrow \eta_b \gamma) = (8.4_{-7.2}^{+18.6}) \times [7.7_{-6.6}^{+17.0}] \times 10^{-4}$, where the upper, central, and lower values correspond to $\Delta m = 60 \text{ MeV}$, 110 MeV , and 160 MeV , respectively. For this bottomonium radiative decay, the decay width $\Gamma(Y \rightarrow \eta_b \gamma)$ is found to be very sensitive to Δm because it is proportional to $(\Delta m)^3$. Our result is to be compared with other model predictions such as $\Gamma(Y \rightarrow \eta_b \gamma) = (3.6 \pm 2.9) \text{ eV}$ [12] from the nonrelativistic effective field theory model, $(33.2 \pm 0.1) \text{ eV}$ [13] and 5.8 eV [14] from the RQM.

V. SUMMARY AND DISCUSSION

In this work, we investigated the weak decay constants and the magnetic dipole $V \rightarrow P\gamma$ decays of heavy-flavored mesons such as $(D, D^*, D_s, D_s^*, \eta_c, J/\psi)$ and $(B, B^*, B_s, B_s^*, \eta_b, Y)$ using the LFQM constrained by the variational principle for the QCD-motivated effective Hamiltonian. The momentum dependent form factors $F_{VP}(q^2)$ for $V \rightarrow P\gamma^*$ decays are obtained in the $q^+ = 0$ frame and then analytically continued to the timelike region by

changing \mathbf{q}_\perp to $i\mathbf{q}_\perp$ in the form factors. The coupling constants $g_{VP\gamma}$, which are needed for the calculations of the decay widths for $V \rightarrow P\gamma$, can then be determined in the limit as $q^2 \rightarrow 0$, i.e. $g_{VP\gamma} = F_{VP}(q^2 = 0)$. Our model parameters obtained from the variational principle uniquely determine the above nonperturbative quantities. This approach can establish the extent of applicability of our LFQM to wider ranging hadronic phenomena.

Our predictions of mass spectra and decay constants for heavy pseudoscalar and vector mesons are overall in good agreement with the available experimental data as well as other theoretical model calculations. Our numerical results of the decay widths for $J/\psi \rightarrow \eta_c \gamma$ and $D^{*+} \rightarrow D^+ \gamma$ fall within the experimental error bars. We also estimate the unmeasured full widths for D^{*0} and D_s^{*+} as $\Gamma_{\text{tot}}(D^{*0}) = (55 \pm 6) \text{ keV}$ and $\Gamma_{\text{tot}}(D_s^{*+}) = (0.19 \pm 0.01) \text{ keV}$, respectively. Our predictions for the branching ratios for the bottomed and bottomed-strange mesons are quite comparable with other theoretical model predictions. For the radiative decay of the bottomonium, we find that the decay widths $\Gamma(Y \rightarrow \eta_b \gamma)$ is very sensitive to the value of $\Delta m = M_Y - M_{\eta_b}$. This sensitivity for the bottomonium radiative decay may help to determine the mass of η_b experimentally. In going beyond the static result to see the momentum dependence of the form factor for $V \rightarrow P\gamma^*$, we find that most results in the heavy flavored sector stand almost unaffected from the recoil effects. However, the form factor $F_{D^{*+}D^+}(q^2)$ seems to give a non-negligible recoil effect about 10% between zero and maximum recoil points, i.e. $F_{D^{*+}D^+}(q_{\text{max}}^2)/g_{D^{*+}D^+\gamma} \approx 1.1$.

Since the form factor $F_{VP}(q^2)$ of vector meson radiative decay $V \rightarrow P\gamma^*$ presented in this work is precisely analogous to the vector current form factor $g(q^2)$ in weak decay of ground state pseudoscalar meson to ground state vector meson, the ability of our model to describe such decay is therefore relevant to the reliability of the model for the weak decay. Consideration on such exclusive weak decays in our LFQM is underway. Although our previous LFQM [15,16] and this analyses did not include the heavy mesons comprising both c and b quarks such as B_c and B_c^* , the extension of our LFQM to these mesons will be explored in our future communication.

ACKNOWLEDGMENTS

This work was supported by a grant from Korea Research Foundation under the contract No. KRF-2005-070-C00039.

[1] S. Godfrey and N. Isgur, Phys. Rev. D **32**, 189 (1985).
[2] N. Barik and P. C. Dash, Phys. Rev. D **49**, 299 (1994).

[3] W. Jaus, Phys. Rev. D **53**, 1349 (1996).
[4] N. R. Jones and D. Liu, Phys. Rev. D **53**, 6334 (1996).

- [5] D. Ebert, R. N. Faustov, and V. O. Galkin, *Phys. Lett. B* **537**, 241 (2002).
- [6] H. G. Dosch and S. Narison, *Phys. Lett. B* **368**, 163 (1996).
- [7] T. M. Aliev, D. A. Demir, E. Iltan, and N. K. Pak, *Phys. Rev. D* **54**, 857 (1996).
- [8] H.-Y. Cheng *et al.*, *Phys. Rev. D* **47**, 1030 (1993).
- [9] P. Colangelo, F. De Fazio, and G. Nardulli, *Phys. Lett. B* **316**, 555 (1993).
- [10] P. Singer and G. A. Miller, *Phys. Rev. D* **33**, 141 (1986); **39**, 825 (1989); G. A. Miller and P. Singer, *Phys. Rev. D* **37**, 2564 (1988).
- [11] J. F. Amundson, C. G. Boyd, I. Jenkins, M. Luke, A. V. Manohar, J. L. Rosner, M. J. Savage, and M. B. Wise, *Phys. Lett. B* **296**, 415 (1992).
- [12] N. Brambilla, Y. Jia, and A. Vairo, *Phys. Rev. D* **73**, 054005 (2006).
- [13] C.-W. Hwang and Z.-T. Wei, hep-ph/0609036.
- [14] D. Ebert, R. N. Faustov, and V. O. Galkin, *Phys. Rev. D* **67**, 014027 (2003).
- [15] H.-M. Choi and C.-R. Ji, *Phys. Rev. D* **59**, 074015 (1999).
- [16] H.-M. Choi and C.-R. Ji, *Phys. Lett. B* **460**, 461 (1999).
- [17] H.-M. Choi, C.-R. Ji, and L. S. Kisslinger, *Phys. Rev. D* **65**, 074032 (2002).
- [18] D. Scora and N. Isgur, *Phys. Rev. D* **52**, 2783 (1995).
- [19] W.-M. Yao *et al.* (Particle Data Group), *J. Phys. G* **33**, 1 (2006).
- [20] G. Bonvicini *et al.*, *Phys. Rev. Lett.* **96**, 022002 (2006).
- [21] O. Aquines *et al.*, *Phys. Rev. Lett.* **96**, 152001 (2006).
- [22] A. Heister *et al.* (ALEPH Collaboration), *Phys. Lett. B* **530**, 56 (2002), and references therein.
- [23] H.-M. Choi and C.-R. Ji, *Phys. Rev. D* **72**, 013004 (2005); **58**, 071901(R) (1998).
- [24] D. Becirevic *et al.*, *Phys. Rev. D* **60**, 074501 (1999).
- [25] C. Aubin *et al.* (HPQCD Collaboration), *Phys. Rev. Lett.* **95**, 122002 (2005).
- [26] S. Narison, *Phys. Lett. B* **520**, 115 (2001).
- [27] G. Cvetic *et al.*, *Phys. Lett. B* **596**, 84 (2004); G.-L. Wang, *Phys. Lett. B* **633**, 492 (2006).
- [28] S. Capstick and S. Godfrey, *Phys. Rev. D* **41**, 2856 (1990).
- [29] D. Ebert, R. N. Faustov, and V. O. Galkin, *Phys. Lett. B* **635**, 93 (2006).
- [30] M. Artuso *et al.* (CLEO Collaboration), *Phys. Rev. Lett.* **95**, 251801 (2005).
- [31] M. Artuso *et al.* (CLEO Collaboration), hep-ex/0607074.
- [32] K. W. Edwards *et al.* (CLEO Collaboration), *Phys. Rev. Lett.* **86**, 30 (2001).
- [33] M. Neubert, V. Rieckert, B. Stech, and Q. P. Xu, in *Heavy Flavours*, edited by A. J. Buras and M. Lindner (World Scientific, Singapore, 1992).
- [34] A. Gray *et al.* (HPQCD Collaboration), *Phys. Rev. Lett.* **95**, 212001 (2005).
- [35] S. Hashimoto, *Int. J. Mod. Phys. A* **20**, 5133 (2005).
- [36] M. Jamin and B. O. Lange, *Phys. Rev. D* **65**, 056005 (2002).
- [37] K. Ikado *et al.* (Belle Collaboration), *Phys. Rev. Lett.* **97**, 251802 (2006).
- [38] J. P. Lansberg and T. N. Pham, *Phys. Rev. D* **75**, 017501 (2007).
- [39] R. L. Thews and A. N. Kamal, *Phys. Rev. D* **32**, 810 (1985).